Accurate Frequency-Domain Modeling and Efficient Circuit Simulation of High-Speed Packaging Interconnects

Wendemagegnehu T. Beyene, *Member, IEEE,* and José E. Schutt-Ainé, *Member, IEEE*

***Abstract*— The paper describes an efficient frequency-domain modeling and simulation method of a coupled interconnect system using scattering parameters. First, low-order rational approximations of the multiport scattering parameters are derived over a wide frequency range using a robust interpolation technique. The method applies frequency normalization, shift, and Householder *QR* orthogonalization to improve the stability and the accuracy when solving the resulting systems of equations. For interconnects characterized with frequency-dependent parasitic parameters, the order of the rational of approximation is reduced by using appropriate reference system. Then, the generated multiport pole-residue models are incorporated into a circuit simulator using recursive convolution. Thus, the method avoids explicit convolution, numerical transform, and artificial filtering of a large number of points that are often necessary in conventional approaches. Examples with experimental and simulated results are given to illustrate the method.**

***Index Terms*— Low-order rational approximation, multiport pole-residue model, recursive convolution.**

I. Introduction

THE signal-integrity analyses of high-speed analog and digital-integrated circuits require the modeling and simulation of systems with coupled transmission lines. As the clock speed and packing density increase, the accurate and efficient modeling and simulation of interconnects become important issues. The delays, losses, and dispersions of interconnects at the chip, module, and board levels have became dominant factors in determining the performance of a system.

Traditionally, a transmission line is modeled by cascading resistors, inductors, and capacitors. This method introduces a large number of nodes that substantially increases the simulation time. These lumped-element circuit models introduce excessive ringing and can give accurate results only within a limited frequency range. The lumped-element circuit models must be supplemented to account for frequency-dependent effects in transmission lines. Lossless and distortionless transmission lines are more accurately simulated in the time domain using the method of characteristics. Although the method of characteristics is extended for lossy lines by using numerical techniques [1], it cannot be easily applied to analyze frequency-dependent behaviors such as skin effects and dispersion.

The most general approach for the simulation of transmission lines is based on the convolution method. The impulse responses of transmission-line systems are used to solve the nonlinear convolution equations governing the interconnects and nonlinear drivers and terminations [2]–[4]. The convolution method requires the inverse transforms and band-limit filtering of a large number of points in order to minimize aliasing and unwanted ringing. This method is computationally expensive. In addition, when the convolution method is applied to low-loss or lossless transmission lines whose time-domain impulse response can be infinite in length, the Gibbs phenomenon and aliasing errors can accumulate leading to convergence and numerical stability problems.

Recently, methods that are based on Padé synthesis have been applied to improve the efficiency of interconnect simulation. Asymptotic waveform evaluation (AWE) and its variants, such as complex frequency hopping (CFH) and Padé via Lanczos (PVL) [5]–[7], have been used successfully to analyze interconnect systems. Typical efficiency gains of two to three orders of magnitude over traditional methods have been reported. The synthesis of transmission lines with long delays using these methods is problematic. The selection of expansion points that guarantee stable Padé approximations of highly coupled interconnects with complex impulse responses is heuristic.

In this paper, we present an efficient frequency-domain modeling technique using scattering parameters. The method is based on a robust rational-approximation algorithm that uses frequency normalization, shift, and Householder *QR* orthogonalization to accurately solve the resulting systems of equations. The method generates multiport pole-residue models whose time-domain response can be efficiently calculated using recursive convolution. In Section II, the scattering parameter formulation of a transmission-line system is described. The multiport scattering parameters of transmission lines are derived from parasitic parameters, measurements, or electromagnetic simulation. In Section III, the scattering matrix is approximated using rational functions. The Householder *QR* othogonalization combined with frequency normalization and frequency shifting is used to calculate the coefficients of the rational function with high accuracy. In Section IV, recursive

Manuscript received February 15, 1997; revised June 14, 1997. This work was supported by AFOSR via the MURI Program under Contract F9620-91-0025 and by the National Science Foundation under Grant NSF EEC 89-43166.

W. T. Beyene is with Hewlett-Packard EEsof Division, Westlake Village, CA 91362 USA.

J. E. Schutt-Ainé is with the Department of Electrical and Computer Engineering, University of Illinois, Urbana, IL 61801 USA.

Publisher Item Identifier S 0018-9480(97)07390-0.

convolution is applied to convert the rational functions into macromodels of multiterminal networks that can be used in circuit simulators. The macromodels of the interconnect system are represented as Norton equivalent circuits using conductances and a time-dependent current sources. This implementation is compatible with conventional time-domain simulators such as SPICE and ASTAP, or with methods based on reduced-order techniques such as AWE, CFH, and PVL. The approach bypasses explicit convolutions, inverse Fourier transforms, and low-pass filtering of a large number of points. In Section V, examples of nonlinear analysis of V-shaped interconnect characterized with measurement data, a lossless coupled line system, and a coaxial cable with skin effect are presented to demonstrate both the efficiency and accuracy of the method. Experimental and computer simulated results are compared.

II. Scattering Parameter Formulation

Although transmission lines are often characterized by fundamental parameters such as characteristic impedance and admittance, the measurements and approximations of these parameters are often difficult and prone to numerical inaccuracies. They take extreme values at integer multiples of a quarter-wavelength. For example, the impedance of a line with no shunt loss tends to infinity at low frequency. However, scattering parameters of the transmission-line system are easier to measure and approximate than characteristic impedance and admittance. The magnitude of the frequency-domain scattering parameter of an interconnect system is limited to one, and by choosing an appropriate reference system, the accuracy of the scattering parameter approximation can even be improved.

The n-port scattering parameters of complex interconnect structures can be obtained from frequency-domain measurements with high accuracy by using one of the commercially available network analyzers. The n-port time-domain impulse response can also be obtained from reflection and transmission measurements using a high-speed oscilloscope with time-domain reflectometer (TDR) and time-domain transmission (TDT) options. It is also possible to calculate the scattering parameters of an arbitrary transmission-line system using full-wave analysis techniques. For example, a finite-different time-domain (FDTD) simulation can generate the time-domain scattering parameters. The corresponding frequency-domain scattering parameters are defined in terms of the Fourier transforms of the time signatures of the incident, reflected, and transmitted waves. Scattering parameters of a transmission-line system can also be derived from parasitic parameters, such as R, L, G, and C, resistance, inductance, conductance, and capacitance per unit length $n \times n$ matrices.

An n-coupled transmission line (shown in Fig. 1) can be characterized by a $2n \times 2n$ scattering matrix. The frequency-domain scattering matrix relates the incident waves to the reflected-wave vectors as

$$\begin{aligned} B_1 &= S_{11}A_1 + S_{12}A_2 \\ B_2 &= S_{21}A_1 + S_{22}A_2 \end{aligned} \tag{1}$$

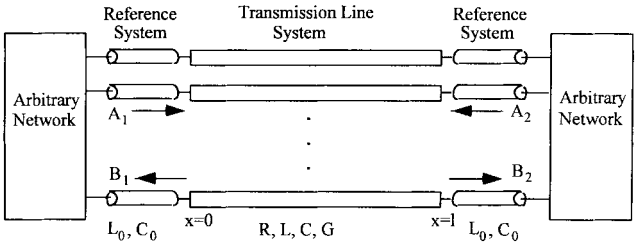

Fig. 1. A network of an n-coupled transmission-line system, reference system, and arbitrary networks.

where S_{ij}'s are $n \times n$ scattering submatrices describing the transmission-line system and A_i's and B_i's are the forward and backward waves, respectively. In order to be able to handle nonlinear devices, the time-domain formulation can be obtained by inverting (1), resulting with the convolution given as

$$\begin{aligned} b_1(t) &= s_{11} * a_1(t) + S_{12} * a_2(t) \\ b_2(t) &= s_{21} * a_1(t) + S_{22} * a_2(t) \end{aligned} \tag{2}$$

where a_i's and b_i's are the time-domain wave vectors associated with A_i's and B_i's, s_{ij}'s are time-domain scattering matrices, and $*$ is used to denote convolution.

For n-coupled transmission lines described by admittance and impedance, $Y(s) = G(s) + sC(s)$ and $Z(s) = R(s) + sL(s)$, respectively, the corresponding multiport scattering matrices can be obtained using the eigenanalysis given in [3]:

$$\begin{aligned} S_{11} = S_{22} &= T^{-1}(\Gamma - \Psi\Gamma\Psi)(1 - \Gamma\Psi\Gamma\Psi)^{-1}T \\ S_{12} = S_{21} &= 2E^{-1}(1 - \Gamma)\Psi(1 - \Gamma\Psi\Gamma\Psi)^{-1}T \end{aligned} \tag{3a}$$

where

$$\begin{aligned} \Gamma &= \left(1 + EE_0^{-1}Z_0H_0H^{-1}Z_m^{-1}\right)^{-1} \\ &\quad \times \left(1 - EE_0^{-1}Z_0H_0H^{-1}Z_m^{-1}\right) \\ T &= \left(1 + EE_0^{-1}Z_0H_0H^{-1}Z_m^{-1}\right)^{-1}E \\ \Psi &= e^{-\Lambda_m l} \end{aligned} \tag{3b}$$

where Z_m and Z_0 are the modal impedances of the transmission line and the associated reference system given by $Z_0 = \Lambda_0^{-1}E_0L_0H_0^{-1}$ and $Z_m = \Lambda_m^{-1}ELH^{-1}$, respectively. The pairs (E, H) and (E_0, H_0) are the left and right eigenvectors matrices associated with diagonal eigenvalue matrices Λ_m and Λ_0 of the interconnect and reference system, respectively, and l is the length of the lines. The parameters of the reference system can be arbitrarily selected. The near-optimal choice of the reference system that give smoother scattering parameters is to make $L_0 = L$ and $C_0 = C$, where L_0 and C_0 are the inductance and capacitance per unit length of the reference system, respectively. In Section III, the approximation of the scattering parameters using rational functions will be described.

III. Rational Approximation

Although the time-domain scattering parameters of interconnect systems can be approximated by a polynomial of exponential functions using such methods as Prony's or the pencil-

of-function, the approximation procedures involve costly nonlinear optimization. Because interconnects are primarily linear and their parameters are simple functions of frequency, they are well characterized in the frequency domain. The frequency-domain approximation is more efficient and can give better results. Hence, the transfer functions of interconnect systems can be approximated by the least maximum error using rational functions.

The scattering parameters $S_{\xi,\vartheta}(j\omega)$ of a linear system can be approximated by a rational function of degree (ξ,ϑ):

$$H_{\xi,\vartheta}(s)=\frac{Q_\xi(s_i)}{P_\vartheta(s_i)}=\frac{q_0+q_1s+q_2s^2+,\cdots,+q_\xi s^\xi}{1+p_1s+p_2s^2+,\cdots,+p_\vartheta s^\vartheta} \quad (4)$$

with p_0 normalized to unity. Equation (4) contains $n=\xi+\vartheta+1$ free coefficients—hence, at most n-independent parameters. The coefficients are determined so that the approximating function evaluated at the same frequency points gives close approximations to the function $S(s)$. For specified finite functional values $y_i=S(s_i)$, $\{i=0,\cdots,k-1\}$, and k specified distinct points, and s_i, the resulting equations, give

$$\frac{Q_\xi(s_i)}{P_\vartheta(s_i)}-y_i=0. \quad (5)$$

By canceling the denominators in (5), one obtains the linear homogenous system of k equations in n unknowns:

$$Q_\xi(s_i)-y_iP_\vartheta(s_i)=0 \quad (6)$$

which can be written in a matrix form, shown in (7) at the bottom of the page.

The columns of $\mathbf{V}\in\mathbf{R}^{k\times n}$ form independent vectors and often $k\geq n$, and (7) is a full-rank overdetermined system. When $k>n$, (7) can be reformulated as a square consistent system that has a unique solution $X=\hat{\mathbf{V}}^{-1}Y$ for any $Y\in\mathbf{R}^n$, where $\hat{\mathbf{V}}\in\mathbf{R}^{n\times n}$ is the reformulated $\mathbf{V}$.

For higher order approximations over a wider approximation range, the system in (7) is highly ill-conditioned and nearly singular because of the large difference between the maximum and minimum frequencies raised to the order of approximation. In [9], partitioned or section-by-section approximation over smaller domains is proposed to avoid the ill-conditioning of the system. The condition number can be improved by normalizing the maximum frequency to unity. The condition number can still be large, though perhaps sufficient for practical purposes, but intolerable for a wide frequency range or high-order approximation. This ill conditioning is real and will not disappear with any further rescaling. On the other hand, posing the problem in a shifted basis normalizes the domain variable around the center of the numerical range within the computer and minimizes numerical inaccuracies in the solution process.

Due to numerical difficulties, solving the consistent equation obtained from (7) using the direct method may give inaccurate results. The problem can be transformed into a more numerically robust equivalent one, yet still produce the solution. Any matrix can be decomposed in the form $\mathbf{V}=\mathbf{QR}$, where $\mathbf{Q}$ is orthogonal and $\mathbf{R}$ is an upper triangular matrix [10]. For a general matrix, the decomposition is constructed by applying a series of Householder reflectors that zero out all elements in a given column to transform the matrix to a triangular form. As in *LU* factorization, Householder *QR* factorization can be obtained in $(n-1)$ steps. However, unlike the Gaussian elimination process, the Householder *QR* decomposition can always be carried out to completion. Thus, the solution of the following triangular system:

$$\mathbf{R}X=\mathbf{Q}^TY \quad (8)$$

is obtained more accurately.

The orthogonal-triangularization method is unconditionally stable—there is a no *growth factor*—the growth of the elements in the reduced matrices are to be considered as in Gaussian elimination. For the ill-conditioned problem, the orthogonal method gives an added measure of reliability. The total computational complexity of the approximation method is one polynomial factorization, two Householder *QR* transformations, and two backsubstitutions. The method with the pseudo-code for the computational procedures are described in detail in [11].

The approximation algorithm can be made more efficient and accurate by utilizing the special properties of the interconnect system fundamental parameters [8]. The functions are analytic functions of a complex variable; hence, their real and imaginary parts are related by Cauchy–Riemann equations. The consequence of this property is that only the real part, imaginary part, angle, or magnitude of the network function has to be approximated and the network function itself can be found from the resulting approximation. The real part of the original scattering matrix is used to determine the denominator polynomial of the rational function. Since the poles are physical attributes of the system, the denominator

$$\underbrace{\begin{bmatrix}1 & s_0 & s_0^2 & \cdots & s_0^\xi & -s_0y_0 & -s_0^2y_0 & \cdots & -s_0^\vartheta y_0\\ 1 & s_1 & s_1^2 & \cdots & s_1^\xi & -s_1y_1 & -s_1^2y_1 & \cdots & -s_1^\vartheta y_1\\ & \vdots & & & & & & & \\ 1 & s_{k-1} & s_{k-1}^2 & \cdots & s_{k-1}^\xi & -s_{k-1}y_{k-1} & -s_{k-1}^2y_{k-1} & \cdots & -s_{k-1}^\vartheta y_{k-1}\end{bmatrix}}_{\mathbf{V}}\times\underbrace{\begin{bmatrix}q_0\\ q_1\\ q_2\\ \vdots\\ q_\xi\\ p_1\\ p_2\\ \vdots\\ p_\vartheta\end{bmatrix}}_{X}=\underbrace{\begin{bmatrix}y_0\\ y_1\\ \vdots\\ y_{k-1}\end{bmatrix}}_{Y} \quad (7)$$

polynomial is common to all scattering parameters. Since the real-part approximation is performed in terms of the squared poles, no unstable right half-plane pole is generated. After removing purely imaginary poles, both real and imaginary parts of the scattering parameters are used to calculate the residues corresponding to the stable poles. The method takes advantage of the reciprocity of the scattering matrix to reduce computation. The scattering parameter is approximated by a stable rational function, whose partial-fraction expansion is given as

$$H(s) = k_\infty + \sum_{i=1}^{\vartheta'} \frac{k_i}{s+p_i}. \tag{9}$$

This partial-fraction expansion is used to characterize the interconnect system. The accuracy of the approximation can be improved by increasing the order of the rational functions, and the condition for passivity $\mathbf{1} - S^*(j\omega)S(j\omega) \geq \mathbf{0}$ can be applied to test the accuracy of the approximation. In Section IV, the partial-fraction expansion is used to perform convolution efficiently to obtain the macromodels of the interconnect system.

IV. Simulation Techniques

The fact was established that the scattering parameters of an interconnect system can be approximated by using a rational function in the frequency domain. Once the partial-fraction expansion of the scattering parameters is obtained, the relation between the incident and the reflected waves is rewritten as

$$B(s) = \underbrace{\left(k_\infty + \sum_{i=1}^{\vartheta} \frac{k_i}{s+p_i}\right)}_{S(s)} A(s) \tag{10}$$

where $A(s)$, $B(s)$, and $S(s)$ are the Laplace-domain incident-, reflected-, and scattering-parameter approximation, respectively. The time-domain response can be obtained by calculating the convolution integral given as

$$b(t) = \int_0^t s(\tau)a(t-\tau)\,d\tau \tag{11}$$

where $a(t)$, $b(t)$, and $s(t)$ are the corresponding time-domain incident, reflected, and scattering parameters, respectively. The convolution integral in (11) becomes progressively more expensive as the time-simulation time increases. Because the scattering parameters are expressed as a sum of partial-fraction expansions (9), the time for the numerical convolution in (11) can be greatly reduced by taking advantage of the recursive convolution.

In 1975, Semlyen and Dabuleanu developed recursive convolution and showed its computational efficiency and usefulness [12]. Recently, recursive convolution is used as an efficient method for transient simulation of transmission lines. It is necessary to make assumptions about the nature of $a(t)$ such that its values at a discrete set of the points suffice to specify $b(t)$ uniquely. As in the backward and forward Euler formulas, the excitation is assumed to be piecewise constant $a(t) = c$ where $t_{n-1} \leq t \leq t_n$ and the equation in (11) is solved using the values of the excitation at the current time interval as boundary conditions

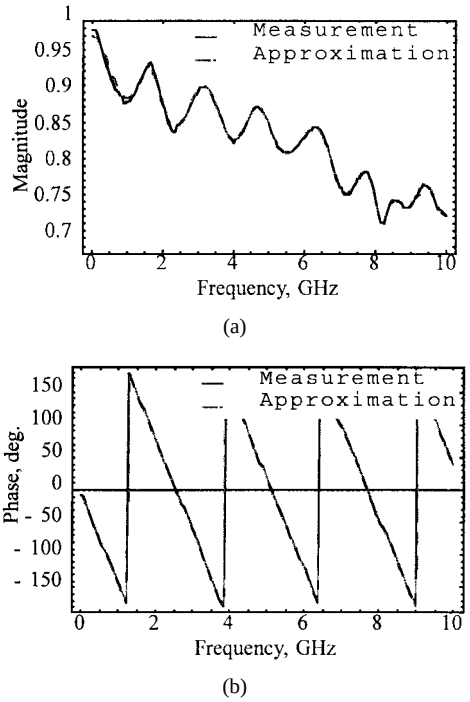

Fig. 2. Example 1. (a) Magnitude and (b) phase plots of S_{12}, the measured data, and the 24th-order rational approximation.

$$b(t_n) = k_\infty a(t_n) + \sum_{i=1}^{q} \tilde{b}_i(t_n) \tag{12}$$

where

$$\tilde{b}_i(t_n) = k_i(1 - e^{-p_i(t_n - t_{n-1})})a(t_{n-1}) + e^{-p_i(t_n - t_{n-1})}\tilde{b}_i(t_{n-1}).$$

Using the recursive convolution formula (12), the convolution in (2) can be reduced into a linear operation that involves a simple update of parameters at each time point. The relationship between a_i's and b_i's is described as

$$\begin{bmatrix} b_1 \\ b_2 \end{bmatrix}_n = \underbrace{\begin{bmatrix} k_\infty^{11} & k_\infty^{12} \\ k_\infty^{21} & k_\infty^{22} \end{bmatrix}}_{K_\infty} \begin{bmatrix} a_1 \\ a_2 \end{bmatrix}_n + \underbrace{\begin{bmatrix} \sum_{i=1}^{q} \tilde{b}^{11} + \sum_{i=1}^{q} \tilde{b}^{12} \\ \sum_{i=1}^{q} \tilde{b}^{21} + \sum_{i=1}^{q} \tilde{b}^{22} \end{bmatrix}_n}_{\tilde{b}_n} \tag{13}$$

where the matrix entries are the coefficients at time-point t_n determined from the pole-residue models of the scattering parameters and the recursive-convolution formula. Because the number of pole-residue pairs is much smaller than the number of time points in the total simulation time, the integration routine is linear in time.

Following the implementation of recursive convolution in [13], the terminal currents and voltages at the transmission-line ports are obtained by writing the incident and reflected waves as

$$a_i = \frac{1}{2}(v_i + Z_0 i_i)$$
$$b_i = \frac{1}{2}(v_i - Z_0 i_i). \tag{14}$$

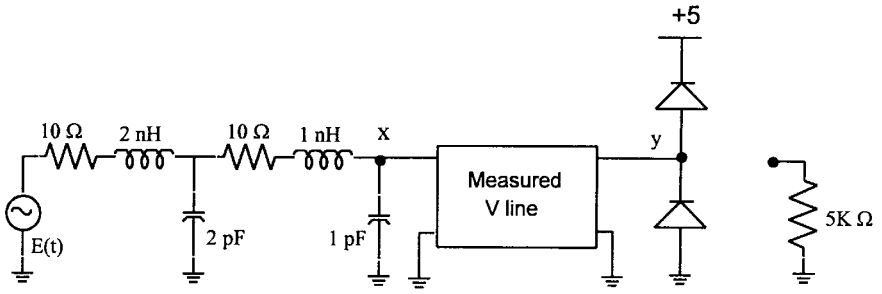

Fig. 3. Example 1. The diode-pair terminated network, (the 5-$k\Omega$ resistor replaces the diode-pair).

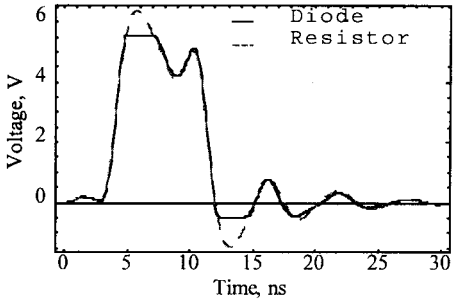

Fig. 4. Example 1. The transient response at node y.

Substituting (14) into (13) at time-point t_n gives the relationship between the terminal voltages and currents as

$$i(t_n) = Z_0^{-1}(1+K_\infty)^{-1}(1-K_\infty)v(t_n) - 2Z_0^{-1}(1+K_\infty)^{-1}\tilde{b}(t_n). \quad (15)$$

Equation (15) can be implemented into circuit simulations as conductance and time-dependent sources. For piecewise constant excitation, the conductance and time-dependent current values are given by

$$G = Z_0^{-1}(1+K_\infty)^{-1}(1-K_\infty)$$
$$J_n = 2Z_0^{-1}(1+K_\infty)^{-1}\tilde{b}(t_n). \quad (16)$$

V. Numerical Results

To verify the capability and to illustrate the advantages of the method, representative examples are presented. Some of the implementation details associated with the method are also described. Experimental and simulated results are compared.

A. Example 1: Measured Interconnect

The scattering parameters of the V-shaped transmission line from [14] are measured in the frequency range 45 MHz–10 GHz with an HP8510B vector network analyzer. The measured scattering parameters of the interconnect are approximated over a frequency range using a rational function. Although the method is able to generate a stable very high-order rational approximation, a 24th- and 27th-order rational function is used to approximate S_{12} and S_{11}, respectively. The magnitude and phase of S_{12} are shown in Fig. 2, respectively. The measured and approximated values are almost indistinguishable.

The proposed method is used to study resistive and diode terminations. The network in Fig. 4 consists of a measured subnetwork, a diode-pair termination, and a resistive termination. The diode is characterized by $i(t) = I_0(\exp(v(t)/v_T - 1)$, where $I_0 = 15$ ps and $v_T = 25$ mV. First, the measured S-parameters are extrapolated to low frequencies for the dc solution. Then, the scattering parameters are incorporated into the system matrix using (16). The network is exited by a pulse with rise and fall times of 0.3 ns and pulse magnitude and width of 5 V and 7 ns, respectively. The network is simulated with the diode-pair termination and with the 5-$k\Omega$ resistor replacing the diodes shown in Fig. 3. The transient responses of the diode-pair termination at node y are compared to those of a 5-$k\Omega$ resistor termination. At the far end, node y, the voltage response of the 5-$k\Omega$ resistor, shows voltage overshoots and undershoots while the diode-pair termination squelch the voltage overshoots, as shown in Fig. 4. Thus, the time-domain analysis of a nonlinear network can be efficiently performed using the proposed method.

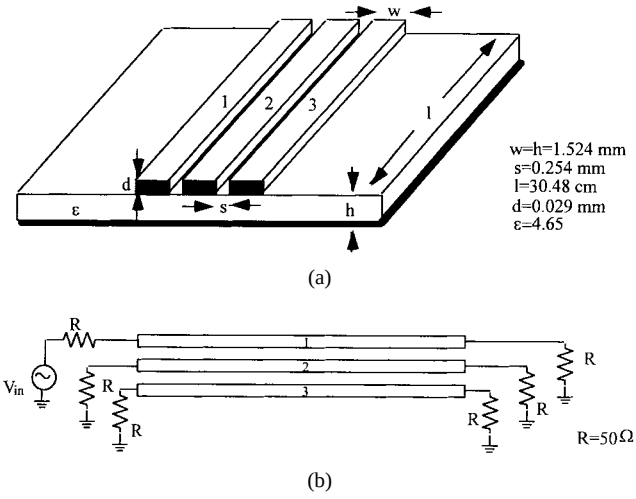

Fig. 5. Example 2. (a) Dimensions of a three-conductor microstrip system. (b) Network of the three-conductor microstrip system.

B. Example 2: Lossless Coupled Transmission Lines

As mentioned in Section I, methods based on convolution have problems dealing with low-loss lines. The situation can lead to an infinite response that results in expensive computation and numerical inaccuracies resulting from the accumulations of errors from convolution and inverse fast Fourier transform (IFFT) of a large number of points. An example of a three-conductor system taken from [15] is shown in Fig. 5. The capacitance and inductance per unit length are,

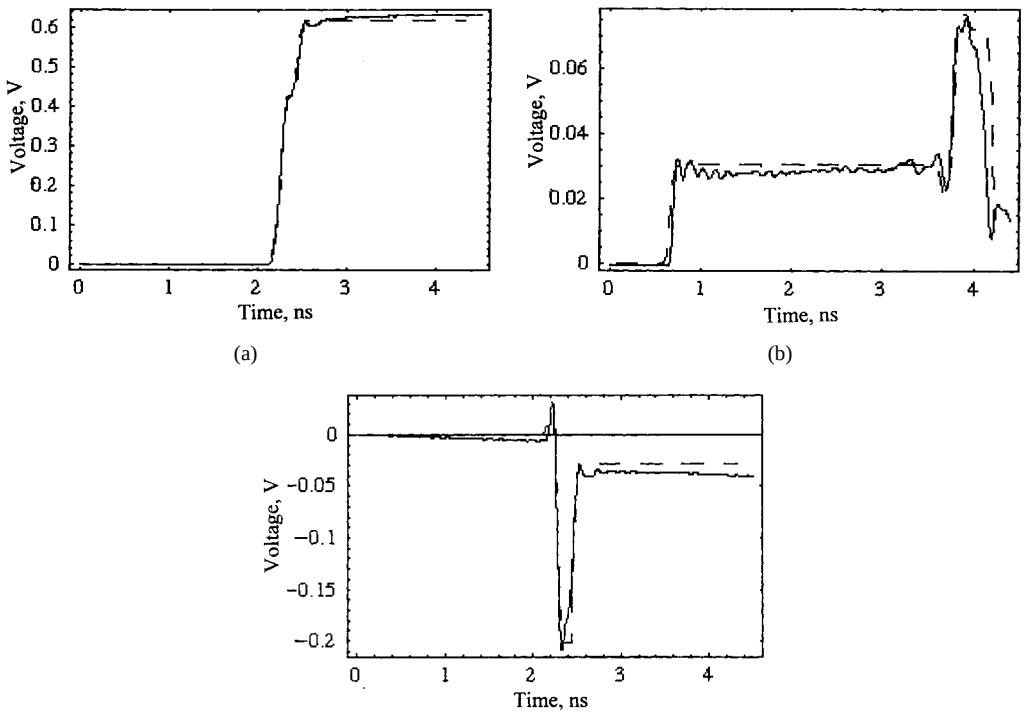

Fig. 6. Measured (solid) and simulated (dashed) voltage waveforms of Example 2. (a) The far end of conductor 1. (b) and (c) The near and far end of conductor 3, respectively.

respectively,

$$C = \begin{bmatrix} 1.0413 & -0.3432 & -0.0140 \\ -0.3432 & 1.1987 & -0.3432 \\ -0.0140 & -0.3432 & 1.0413 \end{bmatrix} \text{ pF/cm}$$

$$L = \begin{bmatrix} 3.8790 & 1.6238 & 0.8252 \\ 1.6328 & 3.7129 & 1.6238 \\ 0.8252 & 1.6238 & 3.8790 \end{bmatrix} \text{ nH/cm} \quad (17)$$

and are simulated using the method. The simulation results are compared with measurement results. The S-parameters are measured using an HP8510B network analyzer with a time-domain option. The 6×6 time-domain impulse-response matrix is integrated with time to obtain the step responses at each port. A very good match between the measurement and simulation for transient responses at the near- and far-end of each line is obtained, as shown in Fig. 6. Some of the spikes are due to unaccounted parasitics of the measurement apparatus.

C. Example 3: The Transient Analysis of Coaxial Cable with Skin Effect

To test the accuracy of the method, the measured and a simulated waveforms of a lossy coaxial line are compared. A 100-m-long coaxial cable has the following characteristic parameters: $L = 476$ nH/m, $C = 0.0476$ nF/m, $G = 0$, and the resistance is characterized with the skin-effect model described as $R(s) = A + B(s)^{\alpha}$, where R is the overall resistance in ohms per meter, $A = 0$, $B = 15.384$, $\alpha = 0.482\,88$, and $s = j2\pi f$, where f is the frequency in gigahertz. The line is not terminated at the far end. A 3-V pulse of 2-ns rise and fall time and a duration of 58 ns is placed at the input in series with 50-Ω source resistance.

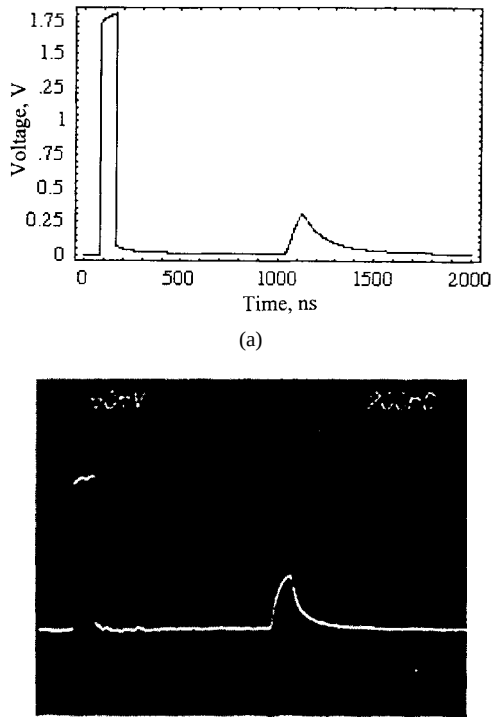

Fig. 7. Example 3. Near end (a) simulated and (b) measured voltage waveforms.

The solutions are compared to time-domain measurement. The simulation and measurement waveforms for near- and far-end ports are identical, as shown in Figs. 7 and 8, respectively.

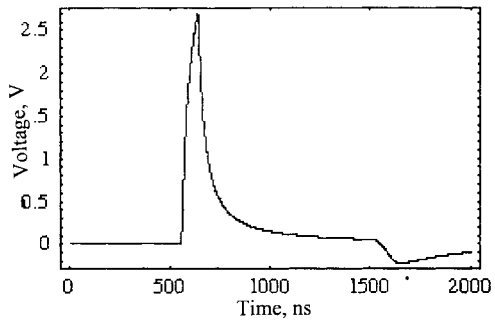

(a)

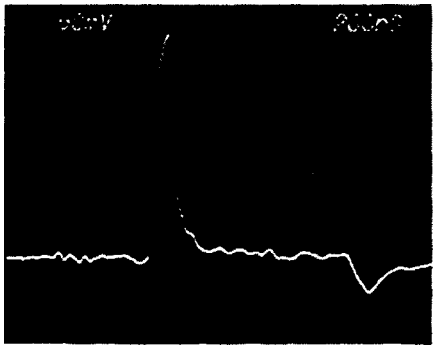

(b)

Fig. 8. Example 3. Far end (a) simulated and (b) measured voltage waveforms.

VI. Conclusion

A robust rational-approximation technique is presented for efficient analysis of an interconnect system with an arbitrary terminal network. The multiport scattering parameters of a coupled interconnect system are derived from frequency-dependent parasitic parameters or given as a table of measured or simulated data. The frequency-dependent scattering matrix characterizing the interconnect system is approximated by rational function, and recursive convolution is used to construct the macromodels that are incorporated into time-domain nonlinear solvers. The macromodels of the interconnects are constructed as Norton-equivalent circuits of conductances and current sources that are updated at each time point. This method allows the analysis of general uniform frequency-dependent interconnects with nonlinear terminations. The method avoids explicit convolution, numerical transform, and artificial filtering of a large number of points that are necessary in conventional approaches. Examples of frequency-dependent interconnects characterized by measurement data and component-based models are given to illustrate the validity and accuracy of the method.

References

[1] N. Orhanovic and V. K. Tripathi, "Nonlinear transient analysis of coupled RLGC lines by the method of characteristics," *Int. J. Microwave Millimeter-Wave CAE*, vol. 2, no. 2, pp. 108–115, 1992.

[2] A. Djordjevic, T. Sarkar, and R. Harrington, "Analysis of lossy transmission lines with arbitrary nonlinear terminations," *IEEE Trans. Microwave Theory Tech.*, vol. MTT-34, June 1986.

[3] D. J. E. Schutt-Ainé and R. Mittra, "Nonlinear transient analysis of coupled transmission lines," *IEEE Trans. Circuits Syst. I*, vol. 36, pp. 959–967, July 1989.

[4] D. Winklestein, M. B. Steer, and R. Pomerleau, "Simulation of arbitrary transmission line networks with nonlinear terminations," *IEEE Trans. Circuits Syst. I*, vol. 38, pp. 418–422, Apr. 1991.

[5] J. Bracken, V. Raghavan, and R. Rohrer, "Interconnect simulation with asymptotic waveform evaluation (AWE)," *IEEE Trans. Circuits Syst. I*, vol. 39, pp. 869–878, Nov. 1992.

[6] E. Chiprout and M. S. Nakhla, "Transient waveform estimation of high-speed MCM networks using complex frequency hopping," in *Proc. Multichip Module Conf. (MCMC)*, Santa Cruz, CA, Mar. 1993, pp. 134–139.

[7] M. Celik and A. C. Cangellaris, "Simulation of dispersive multiconductor transmission lines by Padé approximation via the Lanczos process," *IEEE Trans. Microwave Theory Tech.*, vol. 44, pp. 2525–2535, Dec. 1996.

[8] D. B. Kuznetsov and J. E. Schutt-Ainé, "Optimal transient simulation of transmission lines," *IEEE Trans. Circuits Syst. I*, vol. 43, pp. 111–121, Feb. 1996.

[9] M. Silveira, I. Elfadel, J. White, M. Chilukuri, and K. Kenneth, "Efficient frequency-domain modeling and circuit simulation of transmission lines," *IEEE Trans. Comp., Hybrids, Manufact. Technol.*, vol. 17, pp. 505–513, Nov. 1994.

[11] W. T. Beyene, "Model-order reduction techniques for circuits and interconnects simulation," Ph.D. dissertation, Dept. Elect. Comput. Eng., Univ. Illinois at Urbana-Champaign, 1997.

[12] A. Semlyen and A. Dabuleanu, "Fast and accurate switching transient calculations on transmission lines with ground return using recursive convolutions," *IEEE Trans. Power App. Syst.*, vol. PAS-94, pp. 561–571, Mar./Apr. 1975.

[13] S. D. Corey and A. T. Yang, "Interconnect characterization using time-domain reflectometry," *IEEE Trans. Microwave Theory Tech.*, vol. 43, pp. 2151–2156, Sept. 1995.

[14] J. E. Schutt-Ainé, "Static analysis of V transmission lines," *IEEE Trans. Microwave Theory Tech.*, vol. 40, pp. 2151–2156, Apr. 1992.

[15] F. Y. Chang, "Transient analysis of lossless coupled transmission lines in nonhomogenous dielectric medium," *IEEE Trans. Microwave Theory Tech.*, vol. MTT-18, pp. 616–626, Sept. 1970.

Wendemagegnehu T. Beyene (S'87–M'88), for a photograph and biography, see this issue, p. 1918.

José E. Schutt-Ainé (S'86–M'88) received the B.S. degree from the Massachusetts Institute of Technology (MIT), Cambridge, in 1981, and the M.S. and Ph.D. degrees from the University of Illinois at Urbana–Champaign, in 1984 and 1988, respectively.

He worked for two years with the Hewlett-Packard Microwave Technology Center, Santa Rosa, CA, as a Device Application Engineer. He has also held summer positions at GTE Network Systems, Northlake, IL. He is presently serving on the faculty of the Department of Electrical and Computer Engineering, University of Illinois at Urbana–Champaign, as an Associate Professor. His interests include microwave theory and measurements, electromagnetics, high-speed digital circuits, solid-state electronics, circuit design, and electronic packaging.